Thermal Gap Conductance: Effects of Gas Pressure and Mechanical Load

S. Song*
IBM, Poughkeepsie, New York 12602
and
M. M. Yovanovich† and K. Nho‡
University of Waterloo, Waterloo, Ontario N2L 3G1, Canada

Nitrogen and helium gap-conductance data are reported for interfaces formed by contacting bead-blasted/lapped stainless-steel type 304 and nickel 200 pairs over a range of gas and contact pressures at a fixed mean interface temperature of about 440 K. The effective interface surface parameters are controlled by the bead-blasted surface roughness and mean absolute asperity slope. The effective contact microhardness is controlled by the Vickers microhardness layer of the lapped surface and the effective interface surface parameters. The data show the rarefaction, transition, and continuum heat-conduction regimes at gas pressures from about 10–760 Torr. The predictions of several gap-conductance models are compared against the data. Significant differences between the predictions of some of the models and the data are reported. The models of Veziroglu and Yovanovich are in good to very good agreement with the data.

Nomenclature

A_a = apparent area of contact
A_g = gap area
b_t = surface roughness parameter, $2(CLA_1 + CLA_2)$
CLA = centerline average surface roughness
c_1, c_2 = Vickers microhardness correlation coefficients
d = gap thickness
d_v = Vickers indentation diagonal, μm
H_c = contact microhardness
H_v = Vickers microhardness
h = conductance coefficient, $(Q/A_a)/\Delta T$
h_g^* = dimensionless conductance, $h_g b_t/k_g$
Kn = Knudsen number, Λ/d
k = thermal conductivity, W/m · K
M = gas parameter, $\left(\frac{2-TAC_1}{TAC_1}+\frac{2-TAC_2}{TAC_2}\right)\beta\Lambda$
m = mean absolute asperity slope
P = apparent contact pressure
P_g = gas pressure
Pr = Prandtl number
R_p = maximum peak height
T = temperature, °C
TAC = thermal accommodation coefficient
t = local gap thickness
Q = heat transfer rate
X = dimensionless inverse gas parameter, b_t/M
Y = mean plane separation, effective gap thickness

Greek Symbols

$\alpha = \left(\frac{2-TAC_1}{TAC_1}+\frac{2-TAC_2}{TAC_2}\right)$
$\beta = \frac{2\gamma}{\gamma+1}\frac{1}{Pr}$
γ = ratio of specific heats
ΔT = effective temperature difference across interface
δ = effective gap thickness
Λ = molecular mean-free-path
π = 3.141593
σ = rms surface roughness

Subscripts

0 = reference
1,2 = surfaces 1 and 2
c = contact
g = gap, gas
j = joint

Introduction

HEAT transfer across interfaces formed by contacting metallic surfaces can take place by conduction through the real contact area which consists of numerous microcontacts of different shapes and sizes, by conduction through the substance which fills the gap formed by the contacting solids, and by radiation across the gap when it is filled with a transparent gas or when the contact is made in a vacuum. When the three modes of heat transfer are present at an interface, they are assumed to occur independently and simultaneously, and the joint conductance is set equal to the linear sum of the contact, gap, and radiation conductances (Cetinkale and Fishenden[1] and Yovanovich[2]).

In many practical situations, radiation heat transfer across the gap is negligible relative to conduction heat transfer through the real contact area and the gap; therefore it will be ignored in this paper.

The substance in the gap will be assumed to be either a monatomic or diatomic gas; substances such as liquids or greases will not be considered here.

Presented as Paper 89-0429 at the AIAA 27th Aerospace Sciences Meeting, Reno, NV, Jan. 9-12, 1989; received Feb. 6, 1989; revision received Sept. 25, 1989; accepted for publication Sept. 27, 1989.

*Staff Engineer, Advanced Thermal Technology.
†Director, Microelectronics Heat Transfer Laboratory, Department of Mechanical Engineering. Associate Fellow AIAA.
‡Graduate Research Assistant, Microelectronics Heat Transfer Laboratory, Department of Mechanical Engineering.

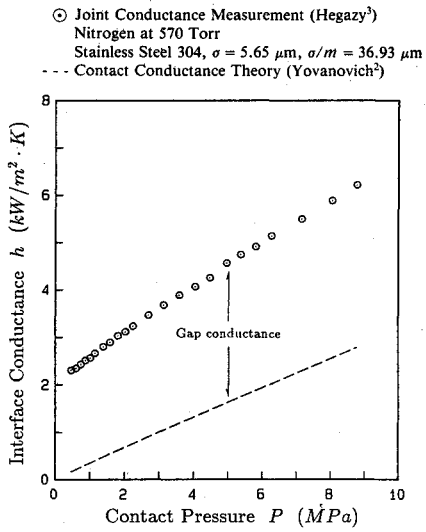

Fig. 1 Gap-conductance contribution to joint conductance.

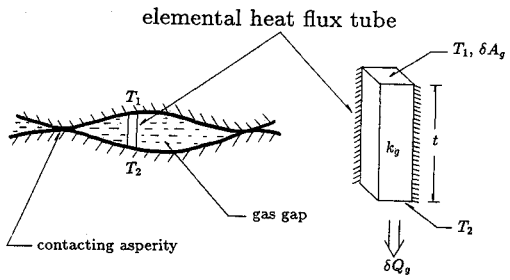

Fig. 2 Elemental heat flux tube.

In nominal applications of contact heat transfer, often the gas conduction through the gap is the predominant mode. The relative magnitude (compared to the contact conductance) of the gap conductance varies greatly depending on contact pressure, microhardness, surface roughness and mean asperity slope, gas pressure and temperature, and the ratio of the thermal conductivity of the gas to those of solids forming the contact.

Typical contributions to the joint conductance of a stainless steel type 304 interface having an effective surface roughness $\sigma = 5.65$ μm with nitrogen at 570 Torr has been reported by Hegazy[3]; they are shown in Fig. 1. At low contact pressure, the contact of the two surfaces is maintained over a very small portion of the apparent area (typically less than 0.01%), and, therefore, the heat transfer takes place mainly through the interstitial gas in the gap. When the contact pressure is 1 MPa, the gap conductance is approximately 92% of the joint conductance. As the contact pressure increases, the contribution of the contact conductance increases and becomes more significant. When the contact pressure is 9 MPa, the gap conductance is seen to contribute approximately 60% to the joint conductance.

The objectives of this paper are 1) to present a brief description of Yovanovich's gap-conductance model, and other available models; 2) to describe an experiment to obtain gap-conductance data for various parameters such as metal and gas properties, smooth and rough surfaces (bead-blasted), and light to moderate contact pressures; and 3) to compare the gap-conductance data against published gap-conductance models.

Gap-Conductance Model by Yovanovich, DeVaal, and Hegazy[4]

Yovanovich and co-workers at the University of Waterloo, assuming a Gaussian surface height distribution, developed a gap-conductance model which accounts for the effect of contact pressure, microhardness, and gas rarefaction effects which appear as separate parameters within an integral. The development of the model is presented briefly here because it will later be used extensively in the present work.

The integral gap-conductance model, which is denoted as the YIGC (Yovanovich integral gap conductance) model, takes the variation in the local gap thickness into consideration due to the surface roughness. The model assumes that the temperatures of the two surfaces in contact are uniform at T_1 and T_2, and that the entire interface gap consists of many elemental flux tubes of different thermal resistance (refer to Fig. 2).

The resistances of these elemental flux tubes are then connected in parallel by an integration over the nominal contact area to result in the overall gap resistance, and by definition the gap conductance is obtained in the form:

$$h_g = \frac{k_g}{\sqrt{2\pi}\sigma}\int_0^\infty \frac{\exp[-(Y/\sigma - t/\sigma)^2/2]}{t/\sigma + M/\sigma}\, d(t/\sigma) \qquad (1)$$

The length scale of the gap is the effective surface roughness σ. The term $(t + M)$ may be regarded as the overall local heat-flow distance of an arbitrary elemental flux tube; it consists of the geometric length t plus the gas rarefaction length M.

The mean plane separation Y is modeled (Yovanovich et al.[4]) as

$$\frac{Y}{\sigma} = \sqrt{2}\,\mathrm{erfc}^{-1}\left(\frac{2P}{H_c}\right) \qquad (2)$$

where the relative contact pressure P/H_c can be estimated (Song and Yovanovich[5]) by

$$\frac{P}{H_c} = \left[\frac{P}{c_1(1.62 \cdot 10^6 \sigma/m)^{c_2}}\right]^{\frac{1}{1+0.071c_2}} \qquad (3)$$

The above expression for the relative contact pressure shows clearly how the effective interface roughness parameter σ/m and the Vickers microhardness data influence the critical load parameter P/H_c.

The gas parameter M has a unit of length and is defined as

$$M = \left(\frac{2 - TAC_1}{TAC_1} + \frac{2 - TAC_2}{TAC_2}\right)\left(\frac{2\gamma}{\gamma + 1}\right)\left(\frac{1}{Pr}\right)\Lambda \qquad (4)$$

The thermal accommodation coefficient TAC depends on the gas/solid combination, and is, in general, sensitive to the condition of the solid surface. It represents the degree to which gas molecules exchange kinetic energy with the solid surface during collisions. TAC for any gas/surface combination may be estimated by the general correlation recently proposed by Song and Yovanovich.[6]

Other Gap Conductance Models

The expressions for various gap-conductance models are summarized in Table 1. Reviews of gap-conductance models may also be found in other references, e.g., Lanning and Hann,[13] Garnier and Begej,[11] and Madhusudana and Fletcher.[14]

It may be noted that the models by Cetinkale and Fishenden,[1] Rapier et al.,[7] Shlykov,[8] and Veziroglu[9] employ a surface roughness parameter b_t as the characteristic roughness. The parameter b_t is defined as

$$b_t = 2(CLA_1 + CLA_2) \qquad (5)$$

The models by Lloyd et al.,[10] Garnier and Begej,[11] and Loyalka[12] make no provision for the estimate of the effective gap thickness δ.

It should also be noted that only the YIGC model accounts for the effect of the mechanical load.

Table 1 Gap-conductance models and correlations

Models	Correlations[a]
Cetinkale and Fishenden[1]	$h_g = \dfrac{k_g}{0.305 b_t + M}$
Rapier et al.[7]	$h_g = k_g\left\{\dfrac{1.2}{2b_t + M} + \dfrac{0.8}{2b_t}\ell_n\left(1 + \dfrac{2b_t}{M}\right)\right\}$
Shlykov[8]	$h_g = \dfrac{k_g}{b_t}\left\{\dfrac{10}{3} + 10\left(\dfrac{M}{b_t}\right) + 4\left(\dfrac{M}{b_t}\right)^2 - 4\left[\left(\dfrac{M}{b_t}\right)^3 + 3\left(\dfrac{M}{b_t}\right)^2 + 2\left(\dfrac{M}{b_t}\right)\right]\ell_n\left(1 + \dfrac{b_t}{M}\right)\right\}$
Veziroglu[9]	$h_g = \dfrac{k_g}{0.264 b_t + M}$, for $b_t > 15$ μm
	$h_g = \dfrac{k_g}{1.78 b_t + M}$, for $b_t < 15$ μm
Lloyd et al.[10]	$h_g = \dfrac{k_g}{\delta + \beta\Lambda/(TAC_1 + TAC_2)}$, δ not given
Garnier and Begej[11]	$h_g = k_g\left\{\dfrac{\exp(-1/Kn)}{M} + \dfrac{1 - \exp(-1/Kn)}{\delta + M}\right\}$, δ not given
Loyalka[12]	$h_g = \dfrac{k_g}{\delta + M + 0.162(4 - TAC_1 - TAC_2)\beta\Lambda}$, δ not given
YIGC model[4]	$h_g = \dfrac{k_g/\sigma}{\sqrt{2\pi}}\displaystyle\int_0^\infty \dfrac{\exp[-(Y/\sigma - t/\sigma)^2/2]}{t/\sigma + M/\sigma}\,\mathrm{d}(t/\sigma)$
	$Y/\sigma = \sqrt{2}\ \mathrm{erfc}^{-1}\left(\dfrac{2P}{H_c}\right)$
	$\dfrac{P}{H_c} = \left[\dfrac{P}{C_1(1.62 \cdot 10^6 \sigma/m)^{C_2}}\right]^{\frac{1}{1 + 0.071 C_2}}$

[a] $b_t = 2(CLA_1 + CLA_2)$, $M = \alpha\beta\Lambda$.

Table 2 Average surface roughness parameters

Experiment number	Specimen number	Surface preparation	σ, μm	CLA, μm	R_p, μm	m	σ/m, μm
1	SS 304[a]	Bead blasted	2.09	1.64	7.77	0.091	22.97
	SS 304	Lapped	0.14	0.1	____	0.023	6.09
2	SS 304	Bead blasted	6.45	5.31	16.7	0.130	49.62
	SS 304	Lapped	0.13	0.1	____	0.020	6.50
3	Ni 200	Bead blasted	11.8	9.68	30.6	0.205	57.56
	Ni 200	Lapped	0.07	0.05	____	0.023	3.04

[a] SS = Stainless steel.

Experimental Apparatus and Test Procedure

Test Apparatus

A Pyrex bell jar and a base plate enclose the test column consisting of the heater block, the heat meter, the upper and lower test specimens, the heat sink, and the load cell. The gas pressure inside the chamber is controlled by the vacuum system which consists of a mechanical pump connected in series with an oil diffusion pump. This system provides a vacuum level lower than 10^{-5} Torr. A brass heater block with two pencil-type heaters provides the maximum total power of 200 W. Cooling is accomplished with an aluminum cold plate which, in turn, is chilled by a closed-loop thermobath. Axial loads up to 4500 N can be applied to the test column through a lever system which is activated by a diaphragm-type air cylinder. The mechanical load is measured by a calibrated load cell. A metal diaphragm type of gauge is used to measure the chamber gas pressure. The uncertainty associated with the gas pressure measurement is ± 0.5 Torr. Temperature measurements were made with 30 gauge-type "T" copper-constantan thermocouples. A more detailed description of the experimental setup is provided in Ref. 3.

Test Specimens

Test specimens of stainless steel type 304 and nickel 200 were prepared from commercial bar stock. The specimens were machined to cylindrical shape of 25 mm diam and 45 mm long. For each specimen, six holes of 0.64 mm diam and 2.5 mm deep were drilled for the thermocouples. These holes were

Table 3 Properties of test gases[a]

Gas	γ	Pr	Λ_o, μm	TAC
Helium	1.67	0.67	0.186	0.55
Nitrogen	1.41	0.69	0.0628	0.78

[a]Note: Λ_o values (Kennard[16]) are at 288 K and 760 Torr. TAC values were estimated according to the method proposed by Song.[15]

located 5 mm apart with the first one 10 mm from the contacting surface.

Upper contacting surfaces were ground, lapped, and finally bead-blasted while lower specimens were ground and lapped. The flatness deviation of the contacting surface of each lapped specimen was checked by means of an optical flat. In general, the deviation was less than 0.3 μm. Talysurf-5 profilometer was employed to measure various surface roughness parameters. The averaged values of measured σ, CLA, R_p (maximum peak height roughness), and m for all test specimens are given in Table 2.

The thermal conductivities of the materials, measured and correlated by Hegazy,[3] are

Stainless Steel 304

$$k(\text{W/m} \cdot \text{K}) = 17.02 + 1.52 \times 10^{-2} T(°\text{C}) \qquad 60°\text{C} \le T \le 250°\text{C} \tag{6}$$

Nickel 200

$$k(\text{W/m} \cdot \text{K}) = 83.15 - 6.56 \times 10^{-2} T(°\text{C}) \qquad 80°\text{C} \le T \le 195°\text{C} \tag{7}$$

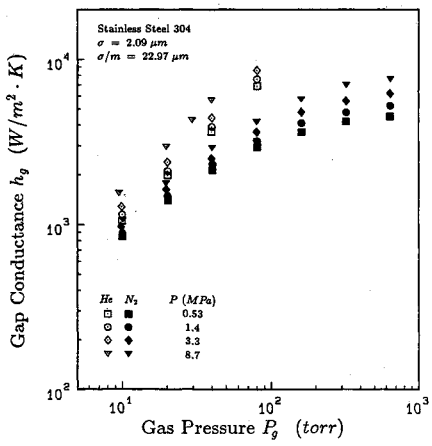

Fig. 3 Gap-conductance results of experiment 1.

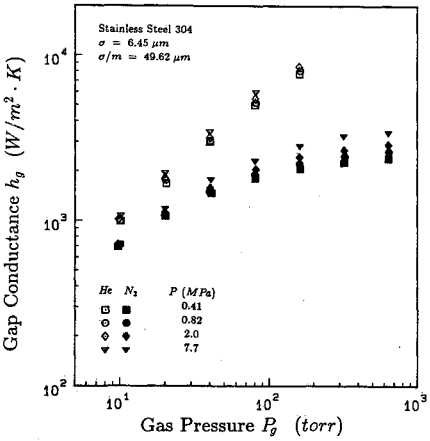

Fig. 4 Gap-conductance results of experiment 2.

The Vickers microhardness measurements were made on the surfaces of the stainless steel and nickel samples, prepared in the same manner as the test specimens. The measurements were correlated to obtain the following expressions (Song[15]):

Stainless Steel 304

$$H_v(\text{MPa}) = 9420 d_v^{-0.330}, \qquad 7\ \mu\text{m} \le d_v \le 60\ \mu\text{m} \tag{8}$$

Nickel 200

$$H_v(\text{MPa}) = 7490 d_v^{-0.321}, \qquad 8.5\ \mu\text{m} \le d_v \le 70\ \mu\text{m} \tag{9}$$

Test Gases

Two significantly different gases, helium and nitrogen, were used in the gap-conductance experiments. Thermal-conductivity correlations developed by Hegazy[3] are used for the test gases:

Helium

$$k_g(\text{W/m} \cdot \text{K}) = 0.145 + 3.24 \times 10^{-4} T(°\text{C}) \qquad 27°\text{C} \le T \le 400°\text{C} \tag{10}$$

Nitrogen

$$k_g(\text{W/m} \cdot \text{K}) = 0.0250 + 5.84 \times 10^{-5} T(°\text{C}) \qquad 27°\text{C} \le T \le 400°\text{C} \tag{11}$$

The values of other relevant properties of the gases, ratio of specific heats, Prandtl number, and molecular mean-free-path are given in Table 3.

Experimental Result

Conductance Measurements

The joint conductance h_j was obtained from the temperature measurements of the test specimens according to its usual definition:

$$h_j = \frac{Q/A_a}{\Delta T} \tag{12}$$

The heat flow rate Q was taken as the average value of the upper and lower test specimens. The interface temperature difference ΔT was obtained from the difference in the extrapolated values of the temperature at the interface obtained from the least-squares-fitted temperature distributions of each test specimen. Gap-conductance data given in the present work are based on the difference of joint conductance values obtained for the gas and vacuum environments. In terms of the gap-conductance coefficients, measured values of h_g correspond to the following:

$$(h_g)_{\text{measured}} = (h_j)_{\text{gas}} - (h_j)_{\text{vacuum}} \tag{13}$$

where $(h_j)_{\text{gas}}$ and $(h_j)_{\text{vacuum}}$ are h_j measurements in a gas environment and in a vacuum, respectively.

This is the most common means by which experimental values of h_g are estimated. The values of h_g obtained according to Eq. (13) most accurately reflect the actual values of h_g when the contribution of the conduction heat transfer through the contacting spots is small compared to that through the gas layer.

For each specimen pair, gap-conductance data were obtained for several mechanical load levels from 0.4–9 MPa. At each load level, the gas pressure was varied from 10–700 Torr. The gap-conductance measurements are shown in Figs. 3–5.

As expected, for a given surface roughness and gas pressure, measurements with helium-filled interfaces show higher gap

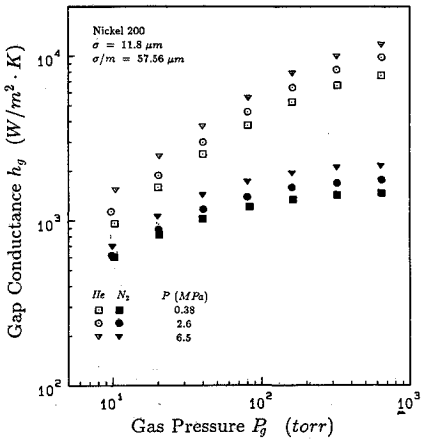

Fig. 5 Gap-conductance results of experiment 3.

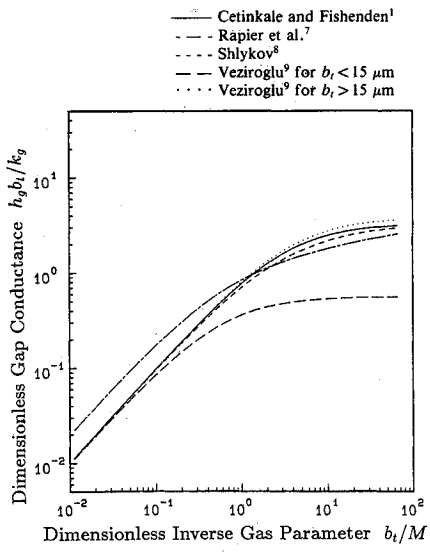

Fig. 6 Comparison of various gap-conductance models.

conductances than those of the nitrogen-filled interfaces. The relative magnitude of gap conductance between the two gases, however, differs according to the gas pressure level. Near the continuum gas conduction regime (high gas pressure), this ratio corresponds to the ratio of the thermal conductivities of the test gases. The effect of gas rarefaction (indicated by the gas pressure dependence) appears on all of the helium measurements, and to a lesser degree on the nitrogen measurements. The gas-rarefaction effect is more significant with the least rough interface.

The effect of mechanical load is shown as an enhancement in the gap conductance, and is more significant near the continuum regime. In Fig. 3, the nitrogen measurement at the gas pressure of 700 Torr shows about 70% increase in the gap conductance due to the mechanical load increase from 0.53–8.7 MPa. When the gas pressure is low, the mechanical load effect is less significant because the gap thickness plays a less important role.

The surface-roughness influence on the measured gap conductances can be clearly seen in Figs. 3–5. For example, the magnitude of the nitrogen gap conductances for the second stainless-steel pair, which has an effective surface roughness three times greater than the first stainless-steel pair, is approximately one-half. Noticeable roughness effects were observed at high gas pressures for nitrogen tests. The lowest gap conductances were obtained with the nickel pair which has an effective surface roughness approximately six or two times larger than the two stainless-steel test interfaces.

Comparison of Various Gap-Conductance Models with Present Experimental Data

In this section, comparisons of various gap-conductance models are made with the present experimental data. Only those models which are for general use and those in which specific expressions for the effective gap thickness are given are considered; i.e., the models proposed by Cetinkale and Fishenden,[1] Rapier et al.,[7] Veziroglu,[9] and Yovanovich's integral gap-conductance model (YIGC) with the Yovanovich-DeVaal-Hegazy[4] estimate of the relative mean plane separation $(Y/\sigma)_{YDH}$. Since the experimental parameter range of the Shlykov's model[8] is similar to that of Cetinkale and Fishenden, only the latter model is considered. It should be noted that Veziroglu's model consists of two expressions: one for moderately rough surfaces ($b_t < 15\mu$m), and the other for very rough surfaces ($b_t > 15\mu$m). The two models of Veziroglu do not give the same gap-conductance values at $b_t = 15$ μm.

Dimensionless Gap-Conductance Parameters

Common to all of these models, with the exception of the YIGC model, is the use of $b_t = 2(CLA_1 + CLA_2)$ as the single parameter for estimating the effective gap thickness. The assumption is that the effective gap thickness is somehow related to the sum of the average roughness heights of the two surfaces. It is important to note that none of these models considers the effect of the mechanical load on the gap thickness, which may be significant when the relative contact pressure is high.

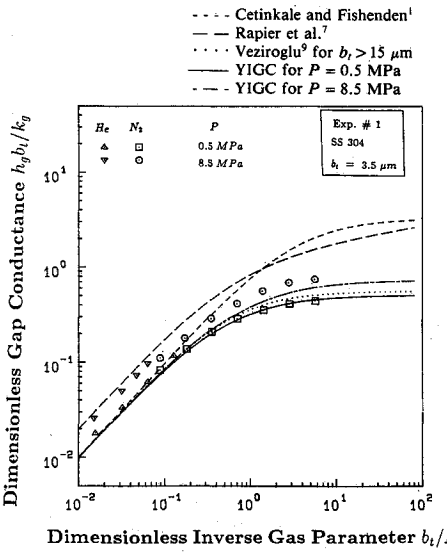

Fig. 7 Comparison of experiment 1 results with various models.

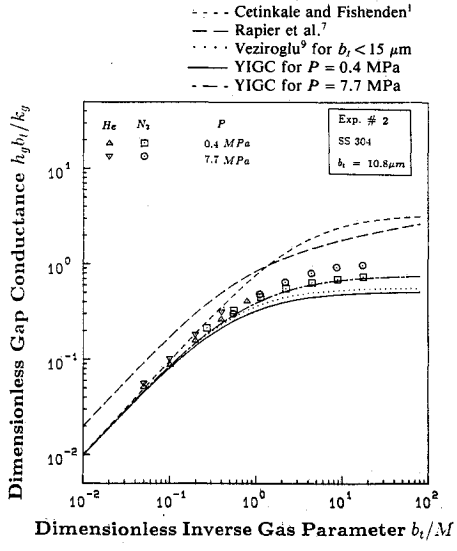

Fig. 8 Comparison of experiment 2 results with various models.

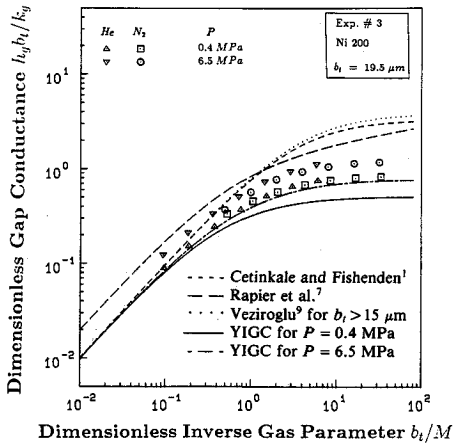

Fig. 9 Comparison of experiment 3 results with various models.

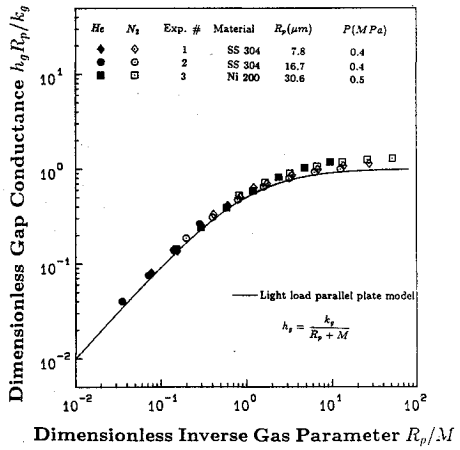

Fig. 10 Comparison of light-load theory with experimental results.

Two dimensionless parameters commonly used by many authors, as discussed by Madhusudana and Fletcher[14,17] are

$$h_g^* = \frac{h_g b_t}{k_g}$$

$$X = \frac{b_t}{M} \tag{14}$$

The parameter h_g^* is the dimensionless gap conductance and X is the dimensionless effective gap thickness which is proportional to the inverse of the gas parameter (or inverse of the temperature jump distance). In terms of these parameters, h_g^* and X, each of the above models, with the exception of the YIGC model, may be expressed by a single curve (two curves for the Veziroglu model) as shown in Fig. 6. The region of low X values represents the rarefied gas heat-conduction regime. As expected in this region, all models, with the exception of Rapier et al.'s, converge to a single curve. This confirms that in the heat-conduction regime where the gas-rarefaction effect dominates, the gap heat transfer is effectively independent of the surface roughness and the gap thickness. Therefore, the ratio h_g/k_g depends only upon the rarefaction parameter M.

Near the continuum regime which is the region of high values of X, these gap-conductance models show considerable disagreement among themselves. It is interesting to observe that the two curves for Veziroglu's model branch out to h_g^* values which differ by an order of magnitude. If a user with surface roughness of $b_t = 15$ μm is to decide upon the choice of the expression from the two Veziroglu models, he or she is to anticipate uncertainties of an order of magnitude in the predicted values of h_g^*.

The significant disagreement among the various models in predicting h_g^* in the near-continuum and continuum regimes is the direct result of their characterizing the effective gap thickness in terms of the roughness parameter b_t which does not account for mechanical load effects.

At the lowest and highest load, helium and nitrogen gap-conductance results of experiment 1 are compared with four models in Fig. 7. The surface pair used in this experiment is relatively smooth ($\sigma = 2.09$ μm, $b_t = 3.5$ μm), and thus the solid conduction contribution to the joint conductance is significant; therefore the uncertainty in the gap-conductance measurements at high load ($P = 8.5$ MPa) and at low gas pressure are large as seen in the helium gap-conductance data which appear to be in good agreement with the Rapier et al.[7] model. Their model does not agree with all other models at low gas pressure. The models of Cetinkale and Fishenden[1] and Rapier et al.[7] significantly overpredict the gap conductance in the continuum regime.

The Veziroglu model[9] for smooth surfaces is in excellent agreement with the light-load helium and nitrogen data, but this model significantly underpredicts the high load/high gas-pressure nitrogen data.

The YIGC model of Yovanovich et al.[4] which accounts for microhardness effects and mechanical loading shows excellent agreement with the light-load helium and nitrogen data over the full gas-pressure range. However, the model appears to underpredict the high-load nitrogen conductance data, but is more accurate than the Veziroglu model.

Figure 8 shows the comparison of the experiment 2 results with four models. The lightest- and highest-load helium and nitrogen gap-conductance data are shown. The data correspond to moderately rough surfaces ($\sigma = 6.45$ μm, $b_t = 10.8$ μm).

The Cetinkale and Fishenden[1] and Rapier et al.[7] models significantly overpredict gap conductances in the near-continuum regime.

The Veziroglu[9] smooth-surface model and the YIGC model for the lightest load are in excellent agreement over the entire range of b_t/M, but are below the lightest-load near-continuum data. The YIGC model predicts the increase expected for the highest load, but it underpredicts the near-continuum gap-conductance results. One observes that the increase in the gap conductance predicted by the YIGC model due to the load change is comparable to the measured increase. With the exception of the Rapier et al.[7] model, all other models agree with the rarefied gas data which show the expected negligible load effect.

Finally, the results of experiment 3, a very rough nickel 200 pair ($\sigma = 11.8$ mm, $b_t = 19.5$ μm) with helium and nitrogen gases, are shown in Fig. 9 at the lowest and highest loads. For this experiment, all three models of Cetinkale and Fishenden,[1] Rapier et al.,[7] and Veziroglu[9] show significant overpredictions. The YIGC model again shows underprediction in the gap conductance. However, it may be noted that the YIGC model predicts well the increase in gap conductance due to the mechanical load increase, and this occurs in the three experiments.

It should be noted that all models with an exception of that of Rapier et al.'s[7] converge to a single curve towards the rarefied gas regime. Near the continuum conduction regime (high b_t/M), the model of Cetinkale and Fishenden[1] and that of Rapier et al.[7] greatly overpredict the contact conductances. Although Veziroglu's model shows better agreement, it does not account for the load dependence.

The YIGC model, for this experiment, underpredicts the gap conductance. The main reason for this appears to be due to the fact that the model assumes the distribution of the asperity heights is Gaussian. Inherent to the Gaussian assumption is that there is no bound for the height of the highest peaks, and, therefore, the YIGC model overestimates the effective gap thickness.

It was shown (Song et al.[18] and Song and Yovanovich[19]) that under a light mechanical load, the effective gap thickness may be estimated by a roughness parameter, the maximum peak height R_p, assuming that measurements of R_p by the profilometer are made over sufficiently long traverse lengths and at different orientations. For this condition, the light-load gap

conductance may be estimated by the parallel-plate-gap model:

$$h_g = \frac{k_g}{R_p + M} \tag{15}$$

The gap conductance and the gas parameter may be normalized using R_p as the characteristic gap thickness to yield

$$\frac{h_g R_p}{k_g} = \frac{1}{1 + M/R_p} \tag{16}$$

Figure 10 shows comparison of this method using R_p at light loads with the light-load data of three experiments. The comparison shows very good agreement. This model underpredicts the data in the continuum regime (high values of R_p/M). As with the other gap-conductance models, it does not account for the mechanical load effect, which is significant. Over the gas-pressure range shown, the normalized gap conductance forms a single curve. This verifies the validity of an accurate estimation of the thermal accommodation coefficients. This observation is consistent with the understanding that for the rarefied gas conduction regime, the heat transfer through the rarefied gas layer is independent of the effective gap thickness.

Summary and Conclusions

The nitrogen and helium gap-conductance data show the effect of the gas and apparent contact pressures and the interface roughness parameters. At the lowest gas pressure of about 10 Torr, both gases show the rarefaction effect, which is greatest with the very rough bead-blasted surfaces. In the rarefaction heat-conduction regime, the gap conductance becomes independent of the mechanical pressure, and it is linearly dependent on the gas pressure.

At the highest gas pressure of about 760 Torr, the nitrogen data show the continuum heat-conduction trend of negligible dependence on gas pressure, but a strong dependence on the surface roughness and the contact pressure.

The helium gap conductance does not show the continuum trend at the highest gas pressure and the roughest surface. The heat transfer occurs entirely in the rarefaction and transition regimes because the accomodation coefficient is small, and the mean-free-path is large.

The helium gap conductances at high gas pressures are seen to be significantly greater than the nitrogen gap conductances, because the thermal conductivity of helium is 6–7 times greater than that of nitrogen.

The gap-conductance models proposed by many researchers show significant differences depending on the gas pressure. When the dimensionless gap conductance based on the b_t scale length is plotted against the dimensionless effective gap thickness b_t/M, one observes that in the rarefaction regime the model of Rapier et al.[7] gives an upper bound, while all other models converge to a common lower bound.

In the continuum regime, the models of Cetinkale and Fishenden,[1] Shlykov,[8] and the second correlation of Veziroglu[9] for $b_t > 15$ μm are nearly the same, and they give the upper bound on the dimensionless gap conductance. The first correlation of Veziroglu[9] for $b_t < 15$ μm and the YIGC model of Yovanovich[4] for light contact pressure are nearly the same, and they give the lower bound. The difference between the upper and lower bounds is almost an order of magnitude for $b_t/M > 10$.

The first correlation of Veziroglu[9] and the YIGC model of Yovanovich[4] are in very good agreement with the data for the smoothest surface at the lightest contact pressure. The YIGC model shows the effect of contact pressure but underpredicts the data. The Veziroglu correlation cannot show the effect of mechanical load.

As the surface roughness increases, the data fall above the Veziroglu and YIGC predictions. However, the YIGC model clearly shows the correct effect of contact pressure.

The second correlation of Veziroglu, which is recommended for the roughest interface, significantly overpredicts the data.

More experimental work is required to understand why the YIGC model, which shows the correct trends with respect to gas and contact pressures effects, underpredicts the data when the contacting surfaces are very rough.

Acknowledgments

The authors acknowledge the financial support of the Natural Sciences and Engineering Research Council of Canada under operating Grant A7455 for Dr. Yovanovich.

References

[1]Cetinkale, T. N., and Fishenden, M., "Thermal Conductance of Metal Surface in Contact," *Proceedings of General Discussion on Heat Transfer,* Inst. of Mechanical Engineering, London, 1951, pp. 271–275.

[2]Yovanovich, M. M., "Thermal Contact Correlations," *Spacecraft Radiative Transfer and Temperature Control,* edited by T. E. Horton, Vol. 83, Progress in Astronautics and Aeronautics, AIAA, New York, 1982.

[3]Hegazy, A. A., "Thermal Contact Conductance of Rough Surfaces: Effect of Surface Micro-Hardness Variation," Ph.D. Dissertation, Dept. of Mechanical Engineering, Univ. of Waterloo, Waterloo, Ontario, Canada, 1985.

[4]Yovanovich, M. M., DeVaal, J. W., and Hegazy, A. A., "A Statistical Model to Predict Thermal Gap Conductance Between Conforming Rough Surfaces," AIAA Paper 82-0888, June 1982.

[5]Song, S., and Yovanovich, M. M., "Relative Contact Pressure: Dependence on Surface Roughness and Vickers Microhardness," *Journal of Thermophysics and Heat Transfer,* Vol. 2, No. 1, 1988, pp. 43–47.

[6]Song, S., and Yovanovich, M. M., "Correlation of Thermal Accommodation Coefficient for 'Engineering' Surfaces," *Fundamentals of Conduction and Recent Developments in Contact Resistance,* edited by M. Imber, G. P. Peterson, and M. M. Yovanovich, American Society of Mechanical Engineers, ASME HTD-Vol. 69, New York, 1987, pp. 117–121.

[7]Rapier, A. C., Jones, T. M., and McIntosh, J. E., "The Thermal Conductance of Uranium Dioxide/Stainless Steel Interfaces," *International Journal of Heat and Mass Transfer,* Vol. 6, 1963, pp. 397–416.

[8]Shlykov, Yu. P., "Calculating Thermal Contact Resistance of Machined Metal Surfaces," *Teploenergetika,* Vol. 12, No. 10, 1965, pp. 79–83.

[9]Veziroglu, T. N., "Correlation of Thermal Contact Conductance Experimental Results," AIAA Paper 67-317, April 1967.

[10]Lloyd, W. R., Wilkins, D. R., and Hill, P. R., "Heat Transfer in Multicomponent Monatomic Gases in the Low, Intermediate, and High-Pressure Regime," Nuclear Thermionics Conf., 1973.

[11]Garnier, J. E., and Begej, S., "Ex-Reactor Determination of Thermal Gap and Contact Conductance Between Uranium Dioxide: Zircaloy-4 Interfaces," U.S. Nuclear Regulatory Commission Rept., 1979.

[12]Loyalka, S. K., "A Model for Gap Conductance in Nuclear Fuel Rods," *Nuclear Technology,* Vol. 57, 1982, pp. 220–227.

[13]Lanning, D. D., and Hann, C. R., "Review of Methods Applicable to the Calculation of Gap Conductance in Zircaloy-Clad UO_2 Fuel Rods," Rept. BNWL-1894, 1975.

[14]Madhusudana, C. V., and Fletcher, L. S., "Gas Conductance Contribution to Contact Heat Transfer," AIAA Paper 81-1163, June 1981.

[15]Song, S., "Analytical and Experimental Study of Heat Transfer Through Gas Layers of Contact Interfaces," Ph.D. Dissertation, Dept. of Mechanical Engineering, Univ. of Waterloo, Waterloo, Ontario, Canada, 1988.

[16]Kennard, E. H., *Kinetic Theory of Gases,* McGraw-Hill, New York, 1938.

[17]Madhusudana, C. V., and Fletcher, L. S., "Solid Spot Thermal Conductance of Zircaloy-2/Uranium Dioxide Interfaces," *Nuclear Science and Engineering,* Vol. 83, 1983, pp. 327–332.

[18]Song, S., Yovanovich, M. M., and Goodman, F. O., "Thermal Gap Conductance of Conforming Surfaces in Contact, Pt. 1: Theory," Tenth Symposium on Thermophysical Properties, Gaithersburg, MD, June 20–23, 1988.

[19]Song, S., and Yovanovich, M. M., "Thermal Gap Conductance of Conforming Surfaces in Contact, Pt. 2: Experimental Results," Tenth Symposium on Thermophysical Properties, Gaithersburg, MD, June 20–23, 1988.